



[Keldysh Institute](#) • [Publication search](#)

[Keldysh Institute preprints](#) • [Preprint No. 2, 2013](#)



[**Zaitsev N.A., Sofronov I.L.**](#)

Grid adaptation for modeling trapezoidal difractors by using pseudo-spectral methods for solving Maxwell equations

Recommended form of bibliographic references: Zaitsev N.A., Sofronov I.L. Grid adaptation for modeling trapezoidal difractors by using pseudo-spectral methods for solving Maxwell equations. Keldysh Institute preprints, 2013, No. 2, 26 p. URL:
<http://library.keldysh.ru/preprint.asp?id=2013-2&lg=e>

**Ордена Ленина
ИНСТИТУТ ПРИКЛАДНОЙ МАТЕМАТИКИ
имени М.В.Келдыша
Российской академии наук**

N.A. Zaitsev, I.L. Sofronov

**Grid adaptation for modeling
trapezoidal difractors by using
pseudo-spectral methods
for solving Maxwell equations**

Москва — 2013

N. A. Zaitsev, I. L. Sofronov, *Grid adaptation for modeling trapezoidal difractors by using pseudo-spectral methods for solving Maxwell equations*

Abstract. We propose a series of successive one-dimensional coordinate transformations to construct an adaptive two-dimensional grid for the problem of diffraction on a grating with a trapezoidal tooth. Special attention is paid to the smoothness of the grid and grid refinement in domains of large solution gradients.

Key words. Adaptive grid, Maxwell equation, diffraction.

Н. А. Зайцев, И. Л. Софронов, *Построение адаптивной сетки для трапециевидных структур при моделировании дифракции псевдо-спектральным методом решения уравнений Максвелла*

Аннотация. В работе предложен ряд последовательных одномерных преобразований координат для построения адаптивной двумерной сетки для задачи дифракции на решетке с трапециевидным зубом. Особое внимание уделено гладкости получаемой сетки и сгущению узлов к местам наибольших градиентов решения.

Ключевые слова: адаптивная сетка, уравнение Максвелла, дифракция.

Contents

I. Preliminaries.....	3
II. Problem formulation.....	4
III. Generation of adaptive z-grid.....	5
IV. Generation of adaptive x-grid	7
V. Numerical examples	13
VI. References	16

I. Preliminaries

We solve 2D diffraction problem described by Maxwell equations

$$\begin{aligned}\frac{1}{c_0} \frac{\partial \vec{D}}{\partial t} &= \nabla \times \vec{H} \\ \frac{1}{c_0} \frac{\partial \vec{H}}{\partial t} &= -\nabla \times \vec{E}\end{aligned}\tag{1}$$

with the dispersion law

$$\begin{aligned}D(r, t) &= \varepsilon_{\infty} E(r, t) + \int_0^t \chi(\tau) E(r, t - \tau) d\tau, \quad r = (x, y, z), \\ \chi(t) &= \sum_{p=1}^P \gamma_p \frac{1}{2i} \left(\exp(-\alpha_p + i\beta_p)t - \exp(-\alpha_p - i\beta_p)t \right).\end{aligned}$$

The scalar p-polarization case of (1), normal incidence, reads:

$$\begin{aligned}\frac{1}{c_0} \frac{\partial D_x}{\partial t} &= -\frac{\partial H_y}{\partial z} \\ \frac{1}{c_0} \frac{\partial D_z}{\partial t} &= \frac{\partial H_y}{\partial x} \\ \frac{1}{c_0} \frac{\partial H_y}{\partial t} &= -\frac{\partial E_x}{\partial z} + \frac{\partial E_z}{\partial x}\end{aligned}\tag{2}$$

Diffraction is considered on a grating with trapezoidal tooth. The pseudo-spectral method [1] used for the solution of this problem requires high-quality grid in this periodical domain. We propose step-by-step method of generating the grid and make analysis of quality of the grid by considering various examples of values of geometric parameters.

II. Problem formulation

Suppose we need to construct computational grid in 2D rectangular computational domain of width W and height H for a periodic with respect to x problem governed by (2). The physical domain is the single spacing of a grating (W coincides with the period of the problem), see Figure 1. The height of the tooth of the grating is h_g and its width is w_g . The angle of the slope of sides of the tooth is α .

Let us introduce the following notations:

x_{\min}, x_{\max} are the horizontal ends of the computational domain, $W = x_{\max} - x_{\min}$;

z_{\min}, z_{\max} are the vertical ends of the computational domain, $H = z_{\max} - z_{\min}$;

z_a is the base of the tooth of the grating;

z_b is the top of the tooth of the grating;

$x_R(z), x_L(z)$ are the right and left supporting lines, see Figure 2. For $z_a < z < z_b$ these lines coincide with the sides of the tooth. One has to continue the lines to the bottom and the top boundaries of the computational domain. They must have vertical tangents at the boundaries in order to use simpler transparent boundary conditions [2].

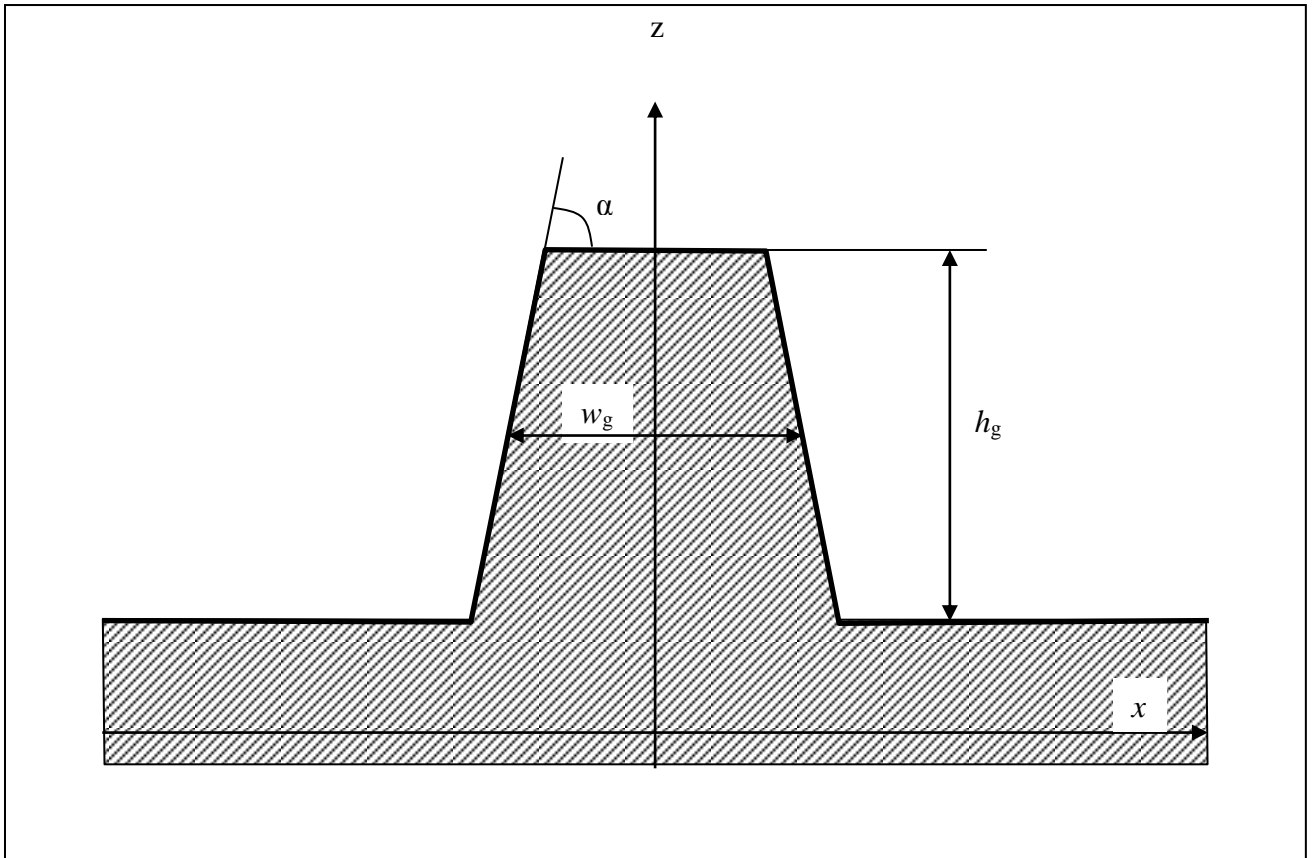


Figure 1. The general view of the computational domain.

III. Generation of adaptive z-grid

We will consider the symmetric case, i.e. when the tooth of the grating is an isosceles trapezoid. In this case

$$\begin{aligned} x_{\max} &= W/2, \quad x_{\min} = -x_{\max}; \quad z_{\max} = H/2, \quad z_{\min} = -z_{\max}; \\ z_b &= h_g/2, \quad z_a = -z_b; \quad x_L(z) = -x_R(z); \\ x_R(z_a) &= (w_g + \cot(\alpha)h_g)/2, \quad x_R(z_b) = (w_g - \cot(\alpha)h_g)/2. \end{aligned}$$

In order to construct adaptive grid and calculate derivatives $\partial/\partial z$ and $\partial/\partial x$ we use a one-to-one map $(x, z) \leftrightarrow (\xi, \zeta)$ such that

$$z = z(\zeta), \quad x = x(\xi, \zeta).$$

We construct the map as a superposition of simpler maps. Let us start from the $z(\zeta)$ transformation.

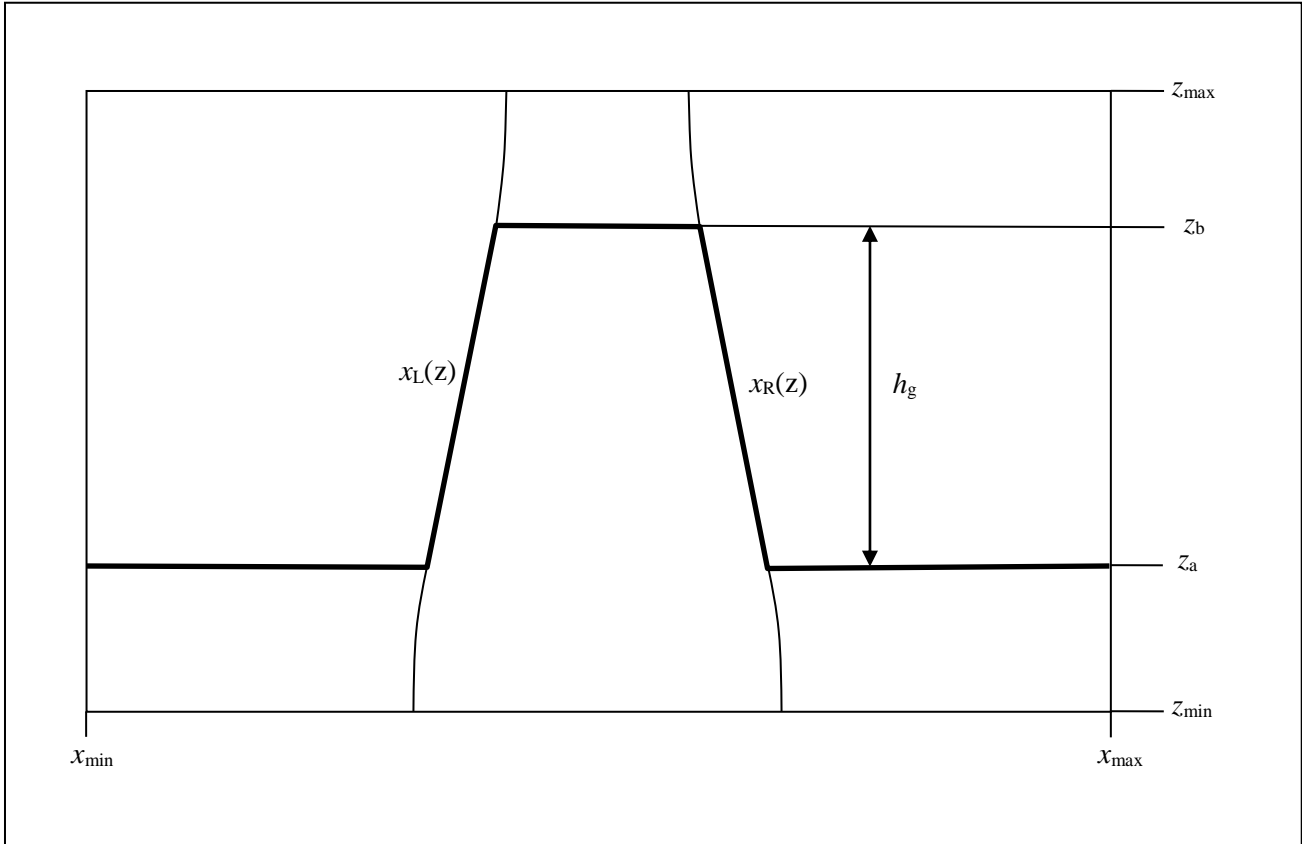


Figure 2. Supporting lines.

In z-direction we have 4 supporting points: z_{\min} , z_a , z_b , z_{\max} . The grid in z-direction should be Chebyshev's type grid and should have small grid spacing near the points z_a and z_b .

First we “normalize” the domain in order to use sine function as a condensing map. So we need to map z_{\min} on -2 , z_a on -1 , z_b on 1 and z_{\max} on 2 . It is done by means of the polynomial function of fifth order:

$$z(\eta) = c_1 \eta + c_5 \eta^5, \quad z_\eta = c_1 + 5c_5 \eta^4, \quad \eta \in [-2, 2] \quad (3)$$

where

$$c_5 = (z_{\max} - 2z_b)/30, \quad c_1 = z_b - c_5.$$

for $z_{\max}/z_b > 1.7$; and by

$$z(\eta) = c_0 \arctan(c_1 \eta), \quad z_\eta = \frac{c_0 c_1}{1 + (c_1 \eta)^2}, \quad \eta \in [-2, 2] \quad (4)$$

where c_0 and c_1 are chosen so that

$$\begin{aligned} c_0 \arctan(c_1) &= z_b, \\ c_0 \arctan(2c_1) &= z_{\max} \end{aligned}$$

for $z_{\max}/z_b < 1.7$.

Now we concentrate grid points to the interfaces $z = z_a$ and $z = z_b$ by means of the following function:

$$\eta(\theta) = 2\theta + (1 - G_z) \sin(2\pi\theta)/\pi, \quad \eta_\theta = 2 + 2(1 - G_z) \cos(2\pi\theta), \quad \theta \in [-1, 1]; \quad (5)$$

where coefficient G_z is the approximate ratio of grid step sizes near the interfaces to sizes of the grid steps without this transformation.

Usually one needs additional transformation in order to redistribute grid points between the inner region $|z| < z_b$ and the outer region $|z| > z_b$. It can be done making use of the following function:

$$\theta(\zeta) = d_1 \zeta + d_3 \zeta^3, \quad \theta_\zeta = d_1 + 3d_3 \zeta^2, \quad \zeta \in [-1, 1] \quad (6)$$

where

$$d_1 = \frac{3R_z}{1 + 2R_z}, \quad d_3 = 1 - d_1,$$

here R_z characterizes a coarsening from the centre and is equal to the value of ratio $\theta_\zeta(0)/\theta_\zeta(1)$ (the derivative $d\theta/d\zeta$ at the middle point $\zeta = 0$ is equal to d_1). If z -

grid without transform (6) is equidistant then the ratio of grid steps at the middle point and at the outer boundary is equal to R_z

If $R_z < 1$ then instead of coarsening the transform concentrates grid points to the center.

However, if $R_z > 2$ then map (6) is not one-to-one. In this case we can use the following map:

$$\theta(\zeta) = \zeta + d_0 \sin(\pi\zeta)/\pi, \quad \theta_\zeta = 1 + d_0 \cos(\pi\zeta), \quad \zeta \in [-1, 1] \quad (7)$$

where

$$d_0 = \frac{R_z - 1}{R_z + 1}.$$

Sometimes this transformation is not aggressive enough. Therefore we can use the following instead of (7):

$$\begin{aligned} \theta &= \theta(t(\zeta)), \quad \theta_\zeta = \theta_t t_\zeta, \\ \theta(t) &= t + d_0 \sin(\pi t)/\pi, \quad \theta_t = 1 + d_0 \cos(\pi t), \quad t \in [-1, 1], \\ t(\zeta) &= \zeta + d_0 \sin(\pi\zeta)/\pi, \quad t_\zeta = 1 + d_0 \cos(\pi\zeta), \quad \zeta \in [-1, 1] \end{aligned} \quad (8)$$

where

$$d_0 = \frac{\sqrt{R_z} - 1}{\sqrt{R_z} + 1}.$$

Now one can construct ζ -grid using the Chebyshev's points

$$\zeta_k = \cos(\pi(N_z - k)/(N_z - 1)), \quad k = 1, \dots, N_z$$

and calculate derivative $d/d\zeta$ with the spectral accuracy, see [3].

IV. Generation of adaptive x-grid

The essential difference between x -grid and z -grid is that the problem is periodic in x -direction. Therefore all our maps must be periodic along lines $z = \text{const}$.

We start the constructing of the x -grid from the eliminating of z -dependence of the grid lines. For this purpose we use transform

$$\begin{aligned} x(y, z) &= y + a \sin(\pi y / y_{\max}), & y \in [-x_{\max}, x_{\max}], \\ x_z &= a_z \sin(\pi y / y_{\max}), & x_y = 1 + a \pi \cos(\pi y / y_{\max}) / y_{\max} \end{aligned} \quad (9)$$

where

$$\begin{aligned} a &= \frac{x_R(z) - y_R}{\sin(\pi y_R / y_{\max})}, \quad a_z = \frac{dx_R(z)/dz}{\sin(\pi y_R / y_{\max})}, \\ y_{\max} &= x_{\max}, \quad y_R = h_g/2. \end{aligned} \quad (10)$$

We need also functions $x_R(z)$ and dx_R/dz . The simplest way to continue x_R is using a polynomial of the second order:

$$\begin{aligned} x_R(z) &= a_0 + a_1 z + a_2 z^2, \quad dx_R/dz = a_1 + 2a_2 z, \quad z \in [z_{\min}, z_a], \\ a_2 &= \frac{x_R(z_b) - x_R(z_a)}{z_b - z_a} \frac{1}{2(z_a - z_{\min})}, \quad a_1 = -2a_2 z_{\min}, \quad a_0 = x_R(z_a) - a_1 z_a - a_2 z_a^2, \\ x_R(z) &= b_0 + b_1 z + b_2 z^2, \quad dx_R/dz = b_1 + 2b_2 z, \quad z \in [z_b, z_{\max}], \\ b_2 &= \frac{x_R(z_b) - x_R(z_a)}{z_b - z_a} \frac{1}{2(z_b - z_{\max})}, \quad b_1 = -2b_2 z_{\max}, \quad b_0 = x_R(z_b) - b_1 z_b - b_2 z_b^2. \end{aligned} \quad (11)$$

One can use also polynomials of the third order:

$$\begin{aligned} x_R(z) &= a_0 + a_1 z + a_2 z^2 + a_3 z^3, \quad dx_R/dz = a_1 + 2a_2 z + 3a_3 z^2, \quad z \in [z_{\min}, z_a], \\ a_3 &= \frac{x_R(z_b) - x_R(z_a)}{z_b - z_a} \frac{1}{3(z_a - z_{\min})^2}, \quad a_2 = -3a_3 z_{\min}, \\ a_1 &= -2a_2 z_{\min} - 3a_3 z_{\min}^2, \quad a_0 = x_R(z_a) - a_1 z_a - a_2 z_a^2 - a_3 z_a^3, \\ x_R(z) &= b_0 + b_1 z + b_2 z^2 + b_3 z^3, \quad dx_R/dz = b_1 + 2b_2 z + 3b_3 z^2, \quad z \in [z_b, z_{\max}], \\ b_3 &= \frac{x_R(z_b) - x_R(z_a)}{z_b - z_a} \frac{1}{3(z_b - z_{\max})^2}, \quad b_2 = -3b_3 z_{\max}, \\ b_1 &= -2b_2 z_{\max} - 3b_3 z_{\max}^2, \quad b_0 = x_R(z_b) - b_1 z_b - b_2 z_b^2 - b_3 z_b^3. \end{aligned} \quad (12)$$

and of the fourth order:

$$\begin{aligned} x_R(z) &= a_0 + a_1 z + a_2 z^2 + a_3 z^3 + a_4 z^4, \quad \frac{dx_R}{dz} = a_1 + 2a_2 z + 3a_3 z^2 + 4a_4 z^3, \quad z \in [z_{\min}, z_a], \\ a_4 &= -\frac{x_R(z_b) - x_R(z_a)}{z_b - z_a} \frac{1}{2(z_a - z_{\min})^3}, \quad a_3 = -2a_4(z_a + z_{\min}), \quad a_2 = -3a_3 z_{\min} - 6a_4 z_{\min}^2, \\ a_1 &= -2a_2 z_{\min} - 3a_3 z_{\min}^2 - 4a_4 z_{\min}^3, \quad a_0 = x_R(z_a) - a_1 z_a - a_2 z_a^2 - a_3 z_a^3 - a_4 z_a^4, \end{aligned}$$

$$\begin{aligned}
x_R(z) &= b_0 + b_1 z + b_2 z^2 + b_3 z^3 + b_4 z^4, \quad \frac{dx_R}{dz} = b_1 + 2b_2 z + 3b_3 z^2 + 4b_4 z^3, \quad z \in [z_b, z_{\max}], \\
b_4 &= -\frac{x_R(z_b) - x_R(z_a)}{z_b - z_a} \frac{1}{2(z_b - z_{\max})^3}, \quad b_3 = -2b_4(z_b + z_{\max}), \quad b_2 = -3b_3 z_{\max} - 6b_4 z_{\max}^2, \\
b_1 &= -2b_2 z_{\max} - 3b_3 z_{\max}^2 - 4b_4 z_{\max}^3, \quad b_0 = x_R(z_b) - b_1 z_b - b_2 z_b^2 - b_3 z_b^3 - b_4 z_b^4.
\end{aligned} \tag{13}$$

To provide higher smoothness one can need even the sixth order. Formulas are derived as follows. We introduce auxiliary map

$$s = z - z_{\min}$$

for $z \in [z_{\min}, z_a]$. Then

$$x_R(z(s)) = a_0 + a_4 s^4 + a_5 s^5 + a_6 s^6, \quad dx_R/dz = 4a_4 s^3 + 2a_5 s^4 + 6a_6 s^5, \quad z \in [z_{\min}, z_a] \tag{14}$$

where the coefficients are obtained from solution of system

$$\begin{aligned}
a_0 + a_4 s_a^4 + a_5 s_a^5 + a_6 s_a^6 &= x_R(z_a) \\
4a_4 s_a^3 + 5a_5 s_a^4 + 6a_6 s_a^5 &= \frac{x_R(z_b) - x_R(z_a)}{z_b - z_a} \\
6a_4 s_a^2 + 10a_5 s_a^3 + 15a_6 s_a^4 &= 0 \\
2a_4 s_a + 5a_5 s_a^2 + 10a_6 s_a^3 &= 0
\end{aligned} \tag{15}$$

with $s_a = z_a - z_{\min}$. Similarly, for $z \in [z_b, z_{\max}]$

$$s = z - z_{\max}$$

and

$$x_R(z(s)) = b_0 + b_4 s^4 + b_5 s^5 + b_6 s^6, \quad dx_R/dz = 4b_4 s^3 + 2b_5 s^4 + 6b_6 s^5, \quad z \in [z_b, z_{\max}] \tag{16}$$

where the coefficients are solution of the system

$$\begin{aligned}
b_0 + b_4 s_b^4 + b_5 s_b^5 + b_6 s_b^6 &= x_R(z_b) \\
4b_4 s_b^3 + 5b_5 s_b^4 + 6b_6 s_b^5 &= \frac{x_R(z_b) - x_R(z_a)}{z_b - z_a} \\
6b_4 s_b^2 + 10b_5 s_b^3 + 15b_6 s_b^4 &= 0 \\
2b_4 s_b + 5b_5 s_b^2 + 10b_6 s_b^3 &= 0
\end{aligned} \tag{17}$$

with $s_b = z_b - z_{\max}$.

One can also use the following infinitely smooth continuation of sides of the trapezoid to the boundaries:

$$\begin{aligned} t(z) &= \frac{C_{xR\text{inf}}}{z_{\min}} + \frac{C_{xR\text{inf}}}{z_a}, \quad z \in (z_{\min}, z_a); \\ \frac{dx_R}{dz} &= \frac{x_R(z_b) - x_R(z_a)}{2(z_b - z_a)} (1 + \operatorname{erf}(y(t))); \\ x_R(z) &= x_R(z_a) + \int_{z_a}^z \frac{dx_R}{dz} dz \end{aligned} \quad (18)$$

where the values of the integral have to be computed numerically.

The difference between the variants of $x_R(z)$ is presented in Figure 3.

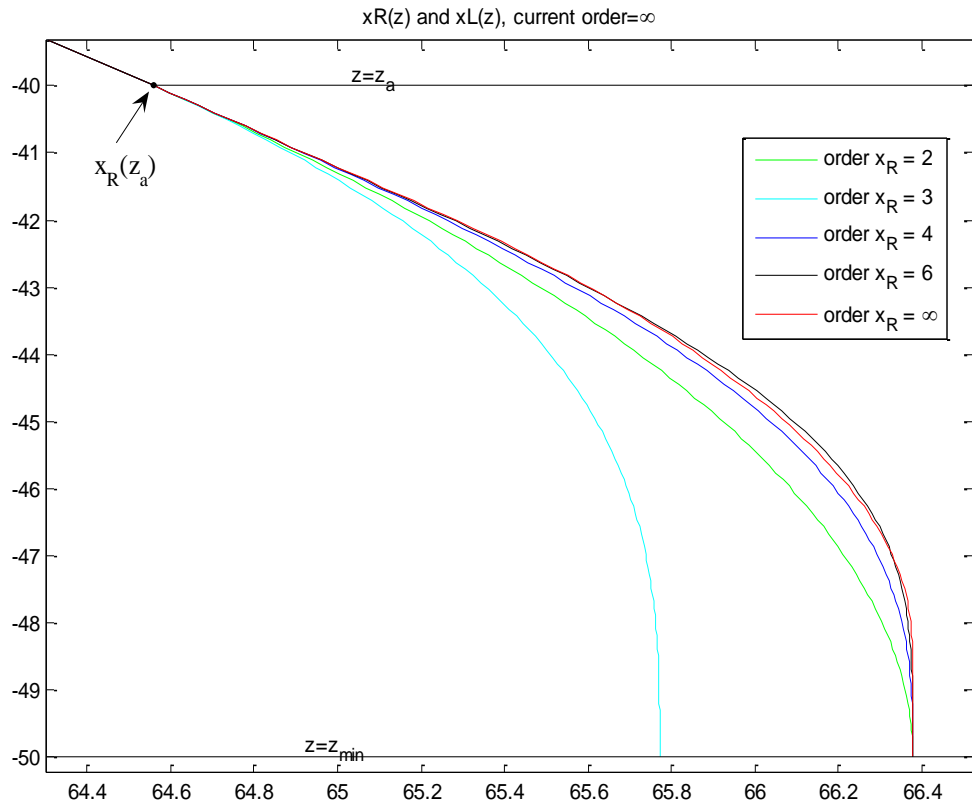


Figure 3. Variants of $x_R(z)$ obtained using polynomials of various orders
in the region $z \in [z_{\min}, z_a]$ (z -axis is vertical)

The dependence of $x_R(z)$ on parameter $C_{xR\text{inf}}$ is as follows: if $C_{xR\text{inf}} \rightarrow \infty$ the curve $x_R(z)$ (red line in Figure 4) tends to the line BED, see Figure 4. In this figure the segment BC is the linear extrapolation of the right side of the trapezoid, the segment ED is the line joining midpoints of sides BC and AC of triangle ABC. If

$C_{xR\inf} \rightarrow 0$ the curve $x_R(z)$ tends to the segment BD. Numerical experiments show that the optimal value of $C_{xR\inf}$ is about π .

One can see that for all the values of parameter $C_{xR\inf}$ point D is the end point of line $x_R(z)$. If we would like to move the end from point D we can use the following function:

$$t(z) = \frac{C_{xR\inf}^{\min}}{z_{\min}} + \frac{C_{xR\inf}^a}{z_a}, \quad z \in (z_{\min}, z_a).$$

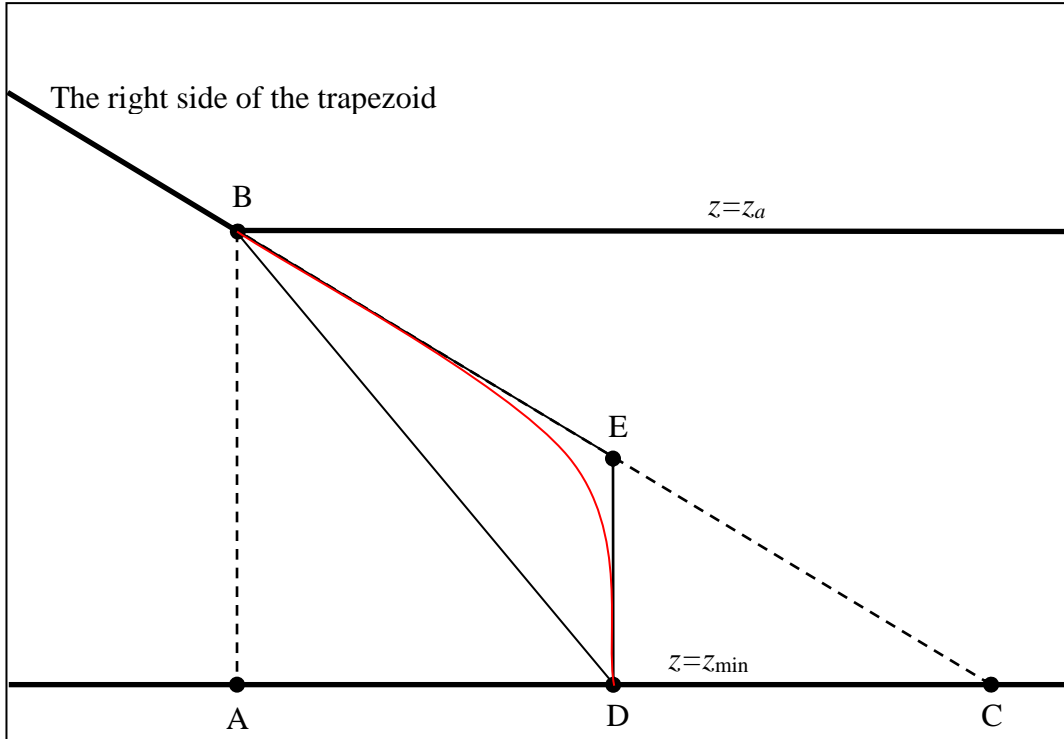


Figure 4. Lay-out of $x_R(z)$

For the interval $z \in [z_b, z_{\max}]$ an infinitely smooth continuation of the sides of the trapezoid is achieved by the following formulas:

$$\begin{aligned} t(z) &= -\frac{C_{xR\inf}}{z_{\max}} - \frac{C_{xR\inf}}{z_b}, \quad z \in (z_b, z_{\max}); \\ \frac{dx_R}{dz} &= \frac{x_R(z_b) - x_R(z_a)}{2(z_b - z_a)} (1 + \operatorname{erf}(y(t))); \\ x_R(z) &= x_R(z_b) + \int_{z_b}^z \frac{dx_R}{dz} dz. \end{aligned} \tag{19}$$

The normalization of the domain $y \in [y_{\min}, y_{\max}]$ we do by the same way as for z-axis. Therefore, we us the map

$$y(\eta) = \frac{y_{\max}}{2}\eta + d_0 \sin\left(\frac{\pi}{2}\eta\right), \quad y_\eta = \frac{y_{\max}}{2} + \frac{d_0\pi}{2} \cos\left(\frac{\pi}{2}\eta\right), \quad \eta \in [-2, 2] \quad (20)$$

where

$$d_0 = y_R - y_{\max}/2$$

for $1.2 < y_{\max}/y_R < 5$ (see (10)); and the map

$$y(\eta) = -y_{\max} + d_0 \int_{-2}^{\eta} \exp\left[d_1 \cos\left(\frac{\pi}{2}t\right)\right] dt, \quad y_\eta = d_0 \exp\left[d_1 \cos\left(\frac{\pi}{2}\eta\right)\right], \quad \eta \in [-2, 2] \quad (21)$$

where parameters d_0 and d_1 must meet the following conditions

$$\begin{aligned} d_0 \int_{-2}^1 \exp\left[d_1 \cos\left(\frac{\pi}{2}\eta\right)\right] d\eta &= y_R + y_{\max}, \\ d_0 \int_{-2}^2 \exp\left[d_1 \cos\left(\frac{\pi}{2}\eta\right)\right] d\eta &= 2y_{\max} \end{aligned}$$

for $y_{\max}/y_R < 1.2$ or $y_{\max}/y_R > 5$.

The following map concentrates grid points to the interfaces $x = x_R(z)$ and $x = x_L(z)$:

$$\eta(\theta) = 2\theta + (1 - G_x) \sin(2\pi\theta)/\pi, \quad \eta_\theta = 2 + 2(1 - G_x) \cos(2\pi\theta), \quad \theta \in [-1, 1] \quad (22)$$

Approximately G_x is the ratio of grid step size near the interfaces to grid steps size without this transformation.

Usually one needs an additional transformation in order to redistribute grid points between the inner region $|x| < x_R(z)$ and the outer region $|x| > x_R(z)$. It can be done by using the following function:

$$\begin{aligned} t(\xi) &= \xi + d_0 \sin(\pi\xi)/\pi, \quad t_\xi = 1 + d_0 \cos(\pi\xi), \quad \xi \in [-1, 1], \\ \theta(t) &= t + d_0 \sin(\pi t)/\pi, \quad \theta_t = 1 + d_0 \cos(\pi t), \quad t \in [-1, 1], \\ \theta_\xi &= \theta_t t_\xi \end{aligned} \quad (23)$$

where

$$d_0 = \frac{\sqrt{R_x} - 1}{\sqrt{R_x} + 1};$$

R_x characterizes the value of ratio $\theta_\xi(0)/\theta_\xi(1)$. If x -grid without transform (23) is equidistant then the ratio of grid steps at the middle point and at the outer boundary is equal to R_x .

However, for big values, if $R_x > 32$, map (23) is not one-to-one. In this case we use the following map:

$$\theta(\xi) = -1 + d_0 \int_{-1}^{\xi} \exp[d_1 \cos(\pi t)] dt, \quad \theta_\xi = d_0 \exp[d_1 \cos(\pi \xi)], \quad \xi \in [-1, 1] \quad (24)$$

where parameters d_0 and d_1 must meet the following conditions:

$$d_1 = \frac{1}{2} \log(R_x),$$

$$d_0 = \frac{2}{\int_{-1}^1 \exp[d_1 \cos(\pi \xi)] d\xi}.$$

Now we can construct equidistant ξ -grid

$$\xi_m = 2m/N_x - 1, \quad m = 1, \dots, N_x$$

($\xi_0 = -\xi_{N_x} = -1$ is excluded because of the periodicity) and calculate derivative $d/d\xi$ with the spectral accuracy, see [3].

V. Numerical examples

In short notation the presented transform has the following form:

$$z = z(\eta^z), \quad \eta^z = \eta^z(\theta^z), \quad \theta^z = \theta^z(\zeta),$$

$$x = x(y, z), \quad y = y(\eta^x), \quad \eta^x = \eta^x(\theta^x), \quad \theta^x = \theta^x(\xi). \quad (25)$$

Thus for a function $u(x, z)$ we have:

$$\begin{aligned}\frac{\partial u}{\partial x} &= \frac{\partial u}{\partial \xi} \left(\frac{\partial x}{\partial \xi} \right)^{-1}, \\ \frac{\partial u}{\partial z} &= \frac{\partial u}{\partial \zeta} \left(\frac{dz}{d\zeta} \right)^{-1} - \frac{\partial u}{\partial \xi} \left(\frac{\partial x}{\partial \xi} \right)^{-1} \frac{\partial x}{\partial z},\end{aligned}\tag{26}$$

where

$$\begin{aligned}\frac{\partial x}{\partial \xi} &= \frac{\partial x}{\partial y} \frac{dy}{d\eta^x} \frac{d\eta^x}{d\theta^x} \frac{d\theta^x}{d\xi}, \quad \frac{dz}{d\zeta} = \frac{dz}{d\eta^z} \frac{d\eta^z}{d\theta^z} \frac{d\theta^z}{d\zeta}, \\ \frac{\partial x}{\partial z} &= \frac{da}{dz} \sin(\pi y / y_{\max}), \quad \frac{da}{dz} = \frac{dx_R(z)}{dz} \frac{1}{\sin(\pi y_R / y_{\max})}.\end{aligned}$$

The corresponding Matlab code which computes the grid and implements formulas (26) has been written.

For numerical tests we take the following function

$$u(x, z) = \exp\left(\frac{z}{z_{\max}}\right) \sin\left(\pi \frac{x}{x_{\max}}\right)\tag{27}$$

for which

$$\frac{\partial u}{\partial z} = \frac{u}{z_{\max}}, \quad \frac{\partial u}{\partial x} = \frac{\pi}{x_{\max}} \exp\left(\frac{z}{z_{\max}}\right) \cos\left(\pi \frac{x}{x_{\max}}\right).\tag{28}$$

In order to check the spectral accuracy of the presented method and its implementation we take the following setup:

$$\begin{aligned}H &= 120, \quad W = 1000, \\ h_g &= 100, \quad w_g = 80, \quad \alpha = 70^\circ;\end{aligned}\tag{29}$$

and the following values of parameters:

$$\begin{aligned}C_{xRinf} &= \pi, \quad G_z = 0.1, \quad G_x = 0.1, \\ z_rarefaction &= 0.125, \quad x_rarefaction = 8.\end{aligned}\tag{30}$$

Table 1 shows obtained accuracy of computed values of $\partial u / \partial z$ and $\partial u / \partial x$ for various numbers of grid points.

Table 1. Error of derivatives versus discretization parameters

N_x	N_z	Error of $\partial u / \partial z$	Error of $\partial u / \partial x$
32	128	2.5×10^{-4}	7.8×10^{-4}
64	256	3.6×10^{-8}	1.7×10^{-7}
128	512	1.7×10^{-12}	4.1×10^{-13}

It's clear that the method has the spectral accuracy.

Nevertheless, it seems that too many points needed to achieve the desired accuracy. The reason is that even a very smooth in (x, z) -space function can have very big gradient in (ξ, ζ) -space. Let us investigate sensitivity to separate parameters of grid. Graph of function $u(x, z)$ (27) in Cartesian coordinates is presented in Figure 5. Graph of the same function in parametric coordinates ξ and ζ for the following values of the parameters

$$\begin{aligned} H &= 120, & W &= 1000, & G_x &= 1, & R_x &= 1, \\ h_g &= 60, & w_g &= 500, & G_z &= 1, & R_z &= 1 \end{aligned} \quad (31)$$

is presented in Figure 6. Here $h_g = H$ and $w_g = W/2$ so the normalization doesn't influence almost. Similar graph for $G_x = 0.1$ is shown in Figure 7. Here $u(\xi, \zeta)$ has much bigger gradient. Change of parameter G_z has similar effect: graph of $u(\xi, \zeta)$ for parameters $G_x = 1$ and $G_z = 0.1$ is shown in Figure 8 (other parameters are not changed). The next Figure shows the picture when we condense grid points to the interfaces in both directions: $G_x = 0.1, G_z = 0.1$.

Graph of $u(\xi, \zeta)$ without any condensation but with coarsening $R_x = 8$ is presented in Figure 10. The same picture with $R_x = 1$ and $R_x = 1/8$ (concentration) is presented in Figure 11. The picture with $R_x = 8$ and $R_x = 1/8$ is presented in Figure 12.

Graph of $u(\xi, \zeta)$ without any condensation and coarsening but for the real positions of the interfaces ($h_g = 100, w_g = 80$) is presented in Figure 13. One can see very strong deformation of the original function (see Figure 6). Graph of $u(\xi, \zeta)$ when all the parameters are active is shown in Figure 14. One can see that the coarsening transform reduces the gradient near the boundaries but generates additional gradient near the center.

Next set of figures shows graphs of correspondent grids.

In Figure 15 and Figure 16 z -grid and its grid steps are shown when there is no coarsening in z direction. Figure 17 and Figure 18 show the same picture for coarsening $R_z = 0.125$.

Figure 19 and Figure 20 show x -grid grid and its grid steps when there is no coarsening in x direction. Figure 21 Figure 22 show the same picture for coarsening $R_x = 8$.

The final grid when all the parameters are active is presented in Figure 23.

VI. References

- [1] Зайцев Н.А., Софронов И.Л. Схемы высокой точности для трёхмерных уравнений Максвелла в средах Лоренца, базирующиеся на неявных схемах переменных направлений // Препринты ИПМ им.М.В.Келдыша. — 2010. — № 79. — 20 с. — URL: <http://library.keldysh.ru/preprint.asp?id=2010-79>
- [2] Софронов И.Л., Воскобойникова О.И., Зайцев Н.А. Прозрачные граничные условия на неравномерных сетках для двумерных уравнений Максвелла с дисперсией Схемы высокой точности для трёхмерных уравнений Максвелла в средах Лоренца, базирующиеся на неявных схемах переменных направлений // Препринты ИПМ им.М.В.Келдыша. — 2011. — № 65. — 20 с. — URL: <http://library.keldysh.ru/preprint.asp?id=2011-65>
- [3] Lloyd N. Trefethen, Spectral Methods in MATLAB, SIAM, Philadelphia, 2000

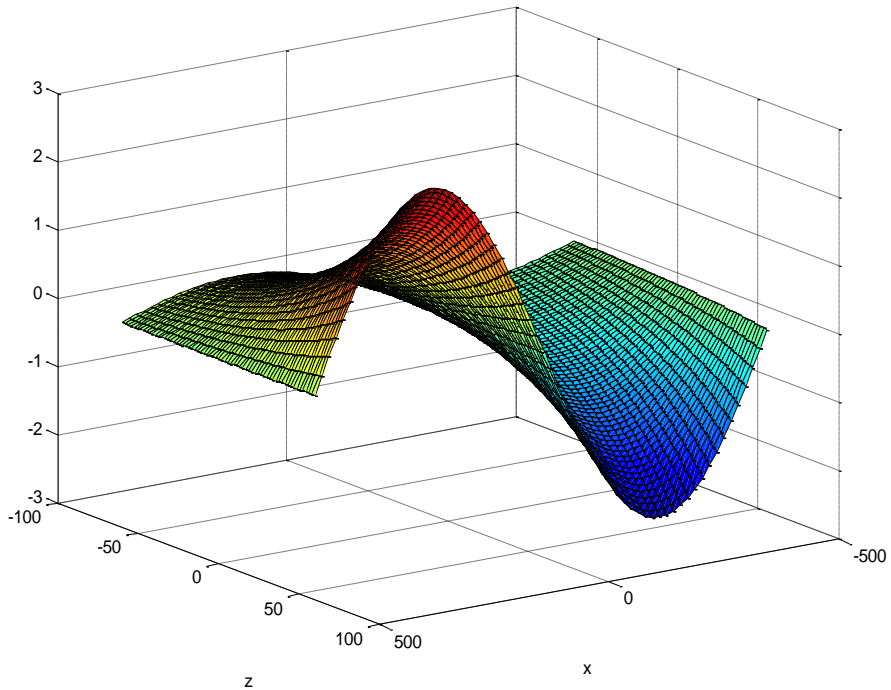


Figure 5. Function $u(x, z)$

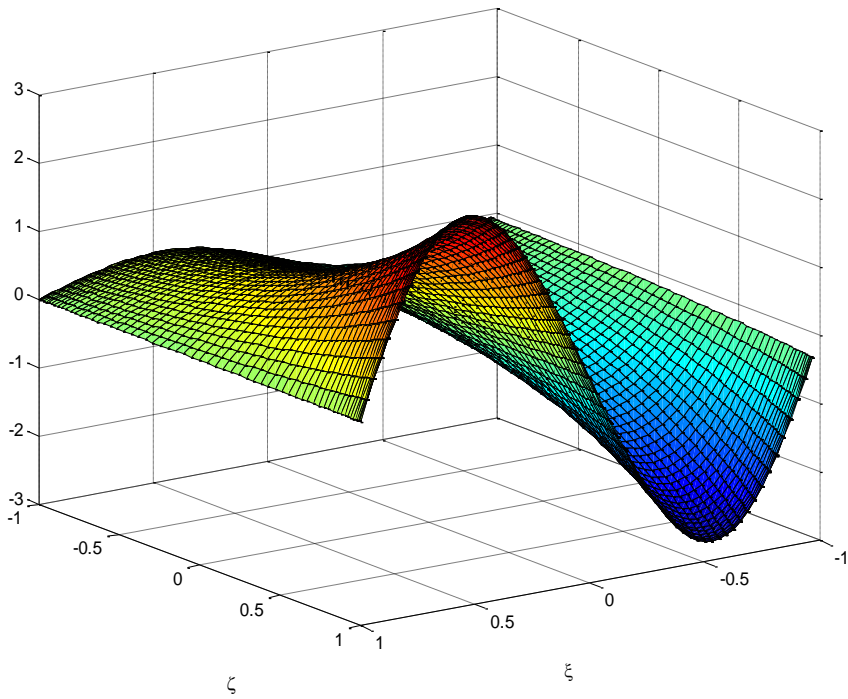


Figure 6. Function $u(\xi, \zeta)$ for parameters of grid transform
 $H=120, h_g=60, W=1000, w_g=500, G_x=1, G_z=1, R_x=1, R_z=1$.

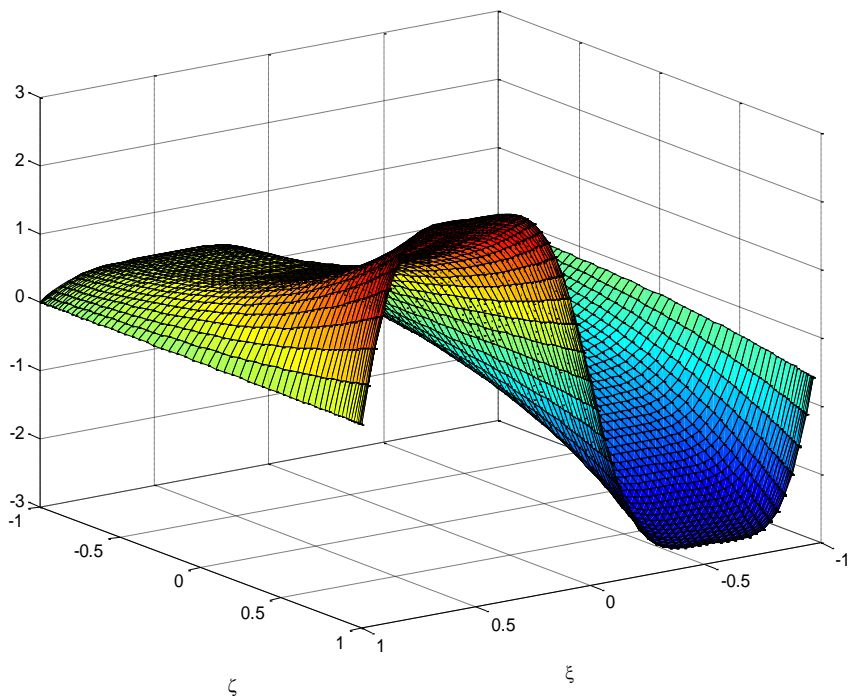


Figure 7. Function $u(\xi, \zeta)$ for parameters of grid transform
 $H = 120, h_g = 60, W = 1000, w_g = 500, G_x = 0.1, G_z = 1, R_x = 1, R_z = 1$.

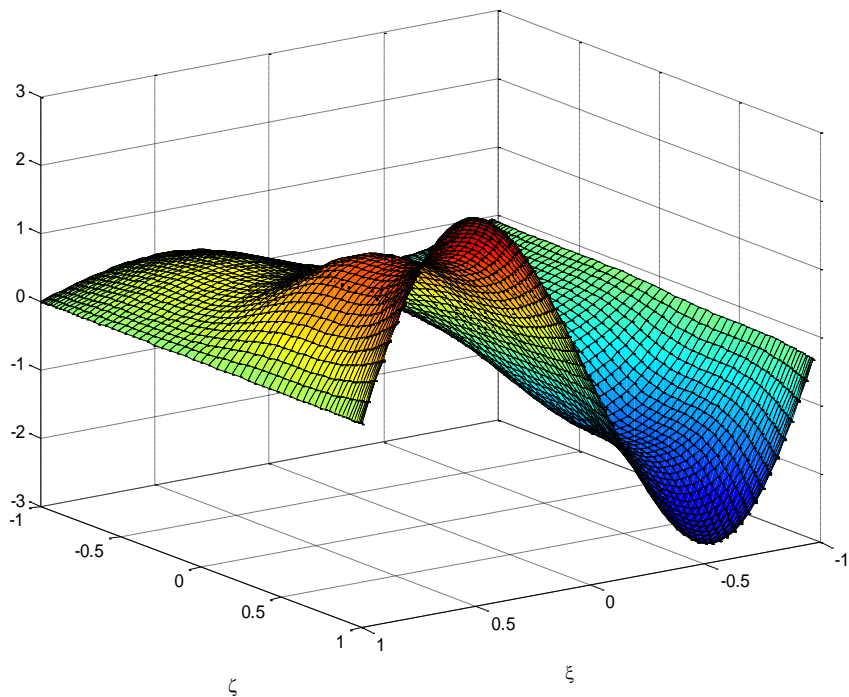


Figure 8. Function $u(\xi, \zeta)$ for parameters of grid transform
 $H = 120, h_g = 60, W = 1000, w_g = 500, G_x = 1, G_z = 0.1, R_x = 1, R_z = 1$.

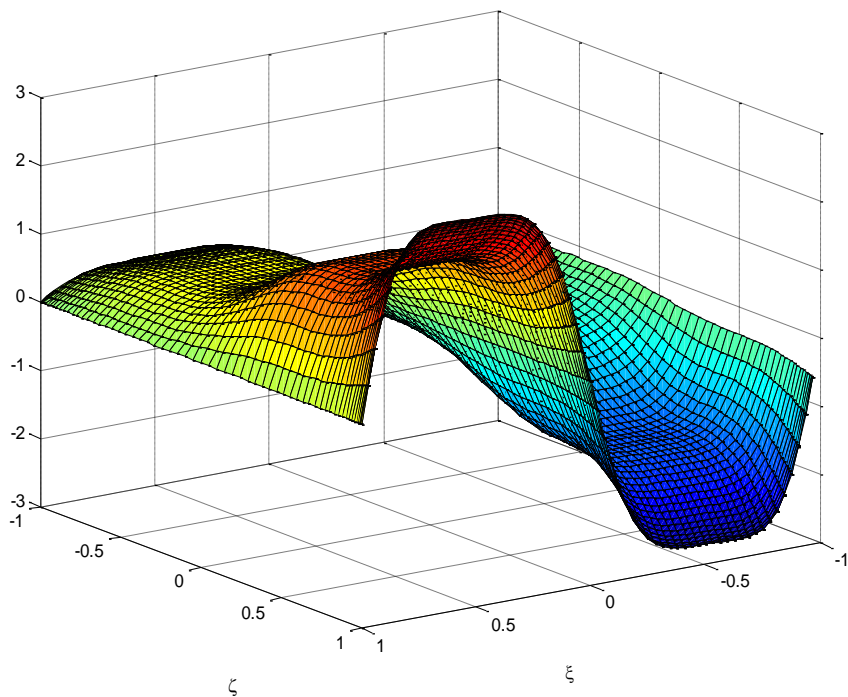


Figure 9. Function $u(\xi, \zeta)$ for parameters of grid transform
 $H = 120, h_g = 60, W = 1000, w_g = 500, G_x = 0.1, G_z = 0.1, R_x = 1, R_z = 1.$

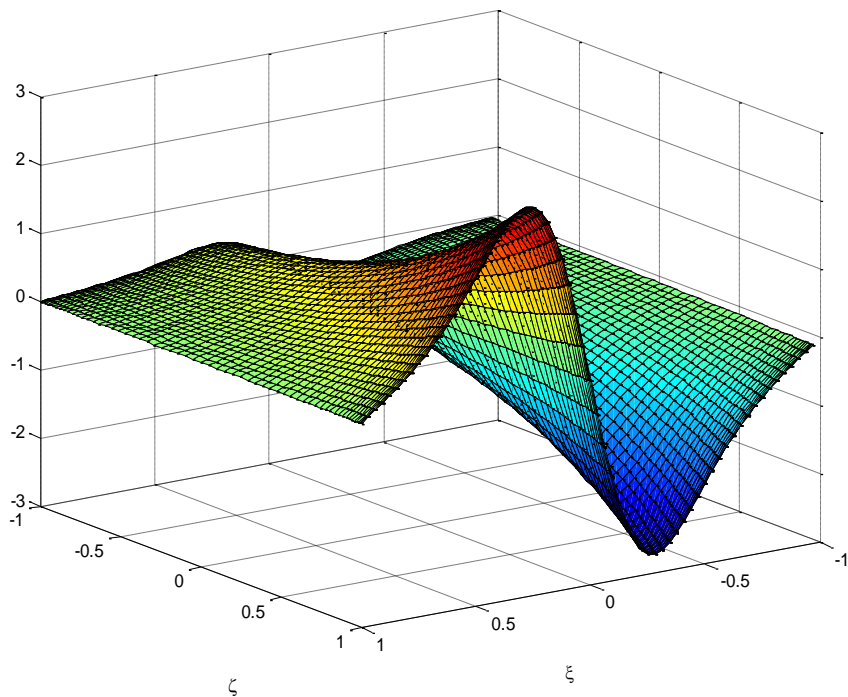


Figure 10. Function $u(\xi, \zeta)$ for parameters of grid transform
 $H = 120, h_g = 60, W = 1000, w_g = 500, G_x = 1, G_z = 1, R_x = 8, R_z = 1.$

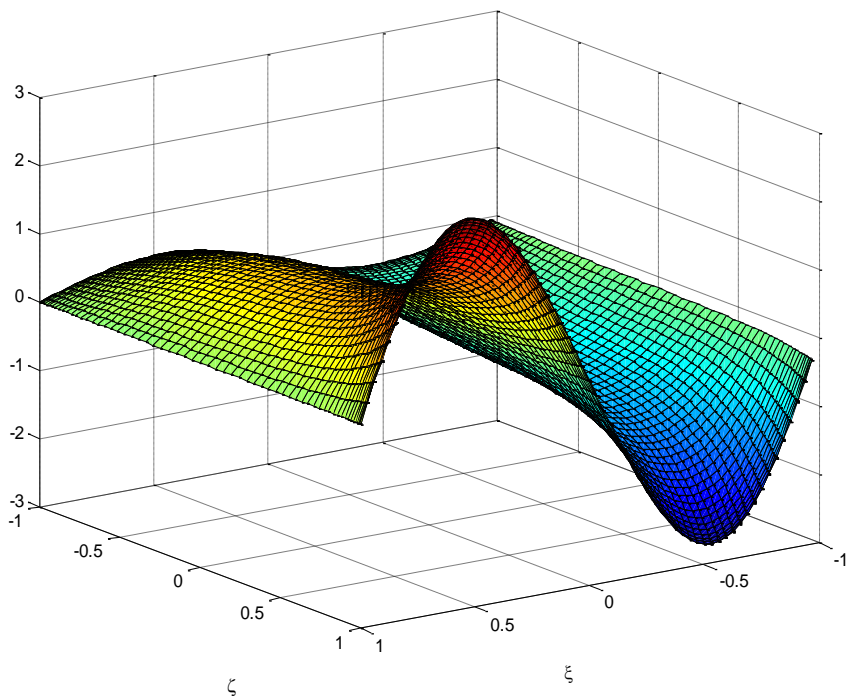


Figure 11. Function $u(\xi, \zeta)$ for parameters of grid transform
 $H = 120, h_g = 60, W = 1000, w_g = 500, G_x = 1, G_z = 1, R_x = 1, R_z = .125$

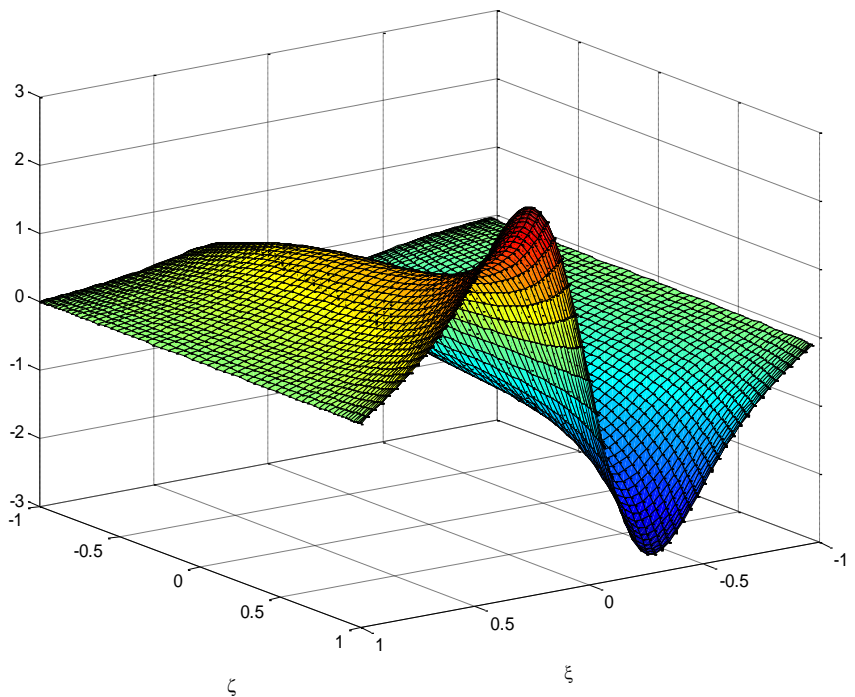


Figure 12. Function $u(\xi, \zeta)$ for parameters of grid transform
 $H = 120, h_g = 60, W = 1000, w_g = 500, G_x = 1, G_z = 1, R_x = 8, R_z = .125$

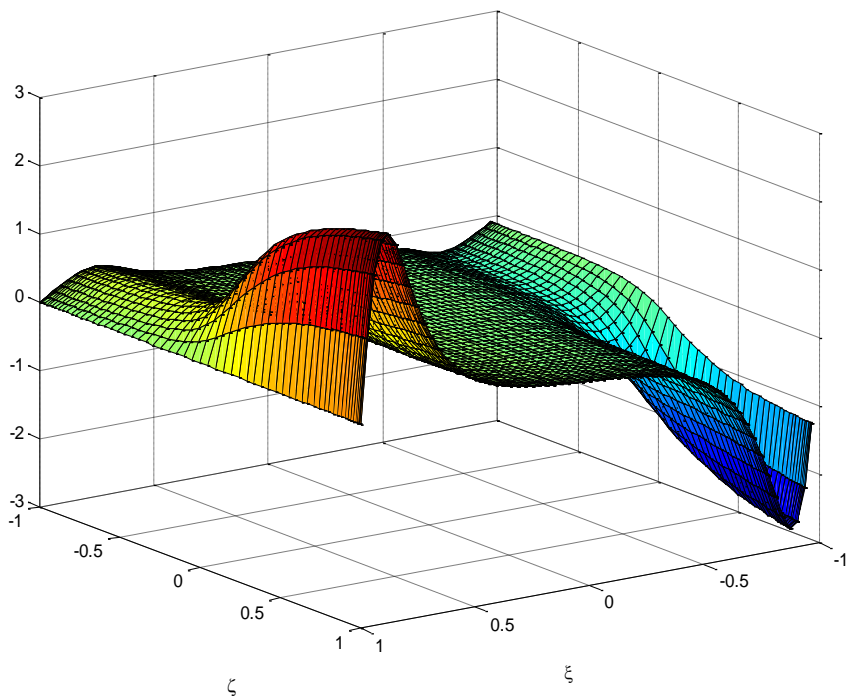


Figure 13. Function $u(\xi, \zeta)$ for parameters of grid transform
 $H=120, h_g=100, W=1000, w_g=80, G_x=1, G_z=1, R_x=1, R_z=1$.

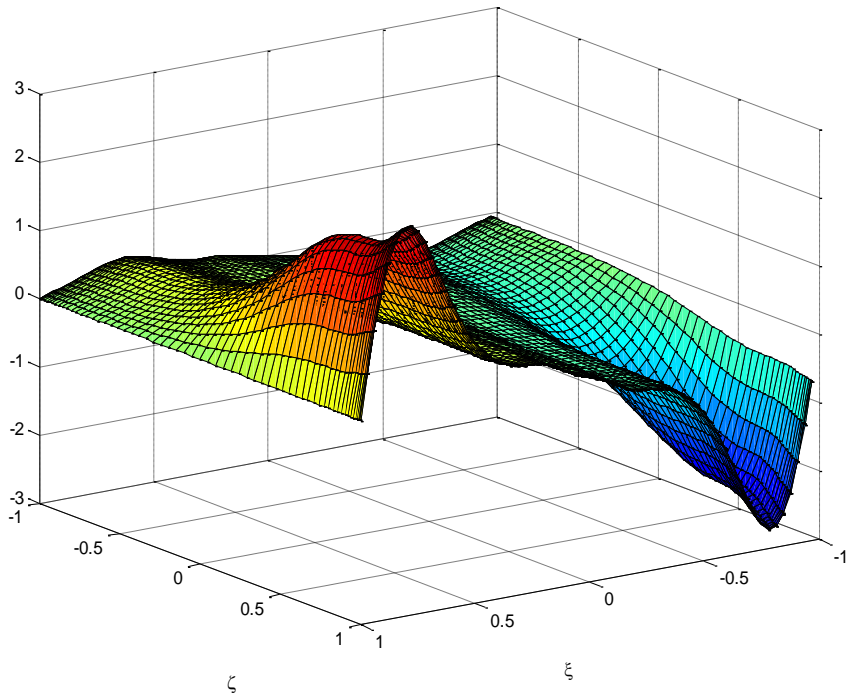


Figure 14. Function $u(\xi, \zeta)$ for parameters of grid transform
 $H=120, h_g=100, W=1000, w_g=80, G_x=.1, G_z=.1, R_x=8, R_z=.125$

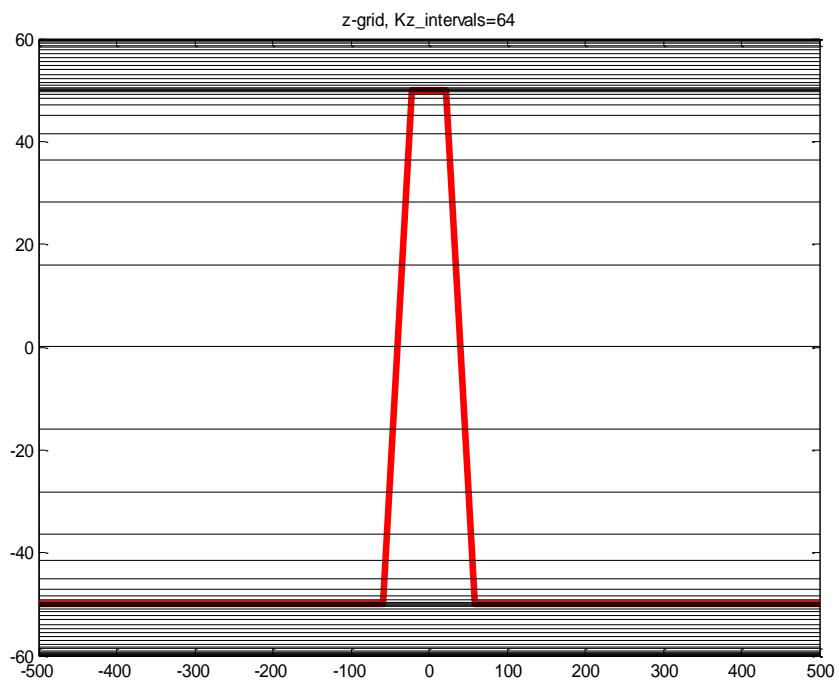


Figure 15. z -grid when there is no coarsening in z direction, $R_z = 1$

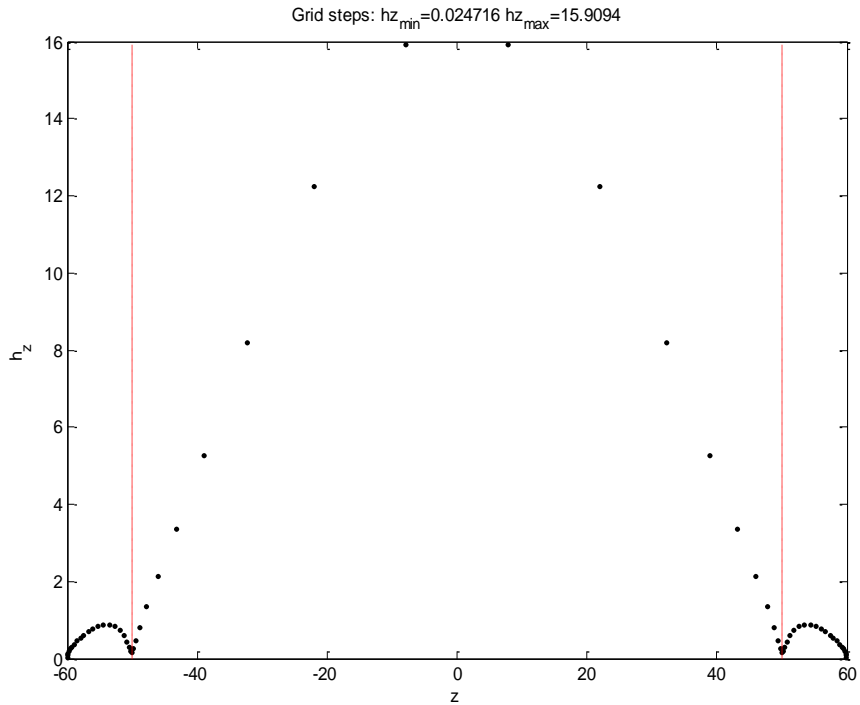


Figure 16. Grid steps $h_z(z)$ when there is no coarsening in z direction, $R_z = 1$

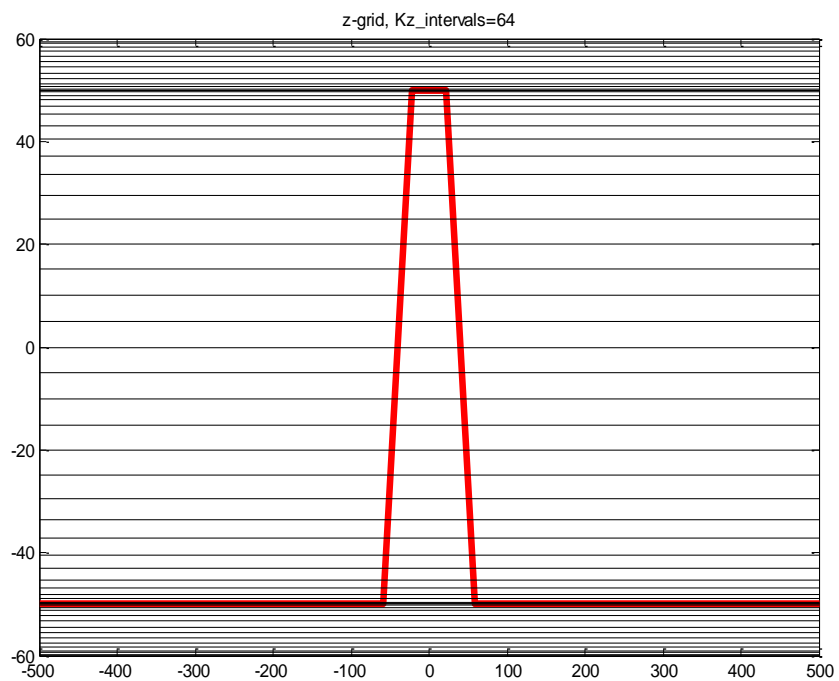


Figure 17. z -grid for coarsening $R_z = 0.125$

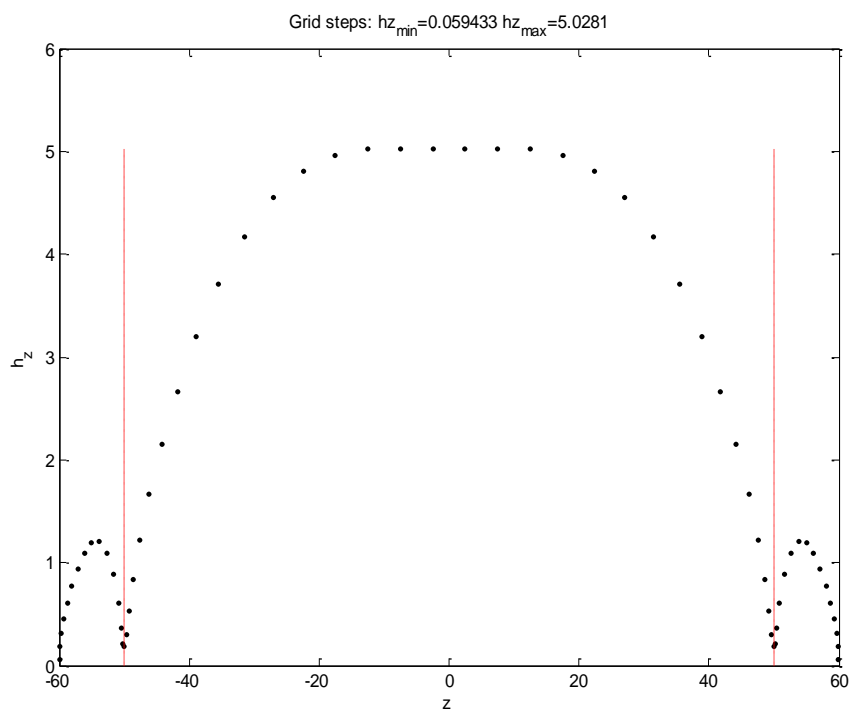


Figure 18. Grid steps $h_z(z)$ for coarsening $R_z = 0.125$

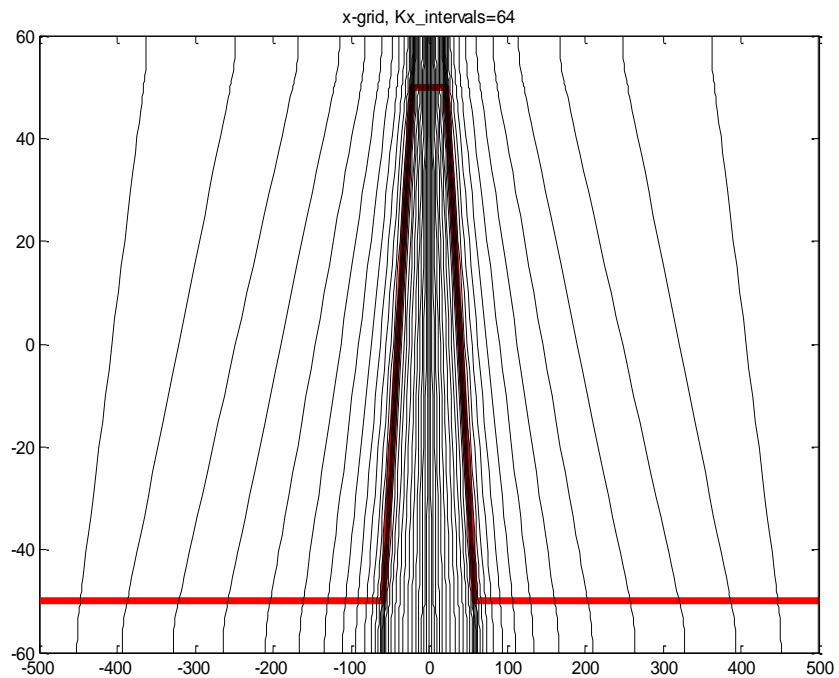


Figure 19. x -grid when there is no coarsening in x direction, $R_x=1$

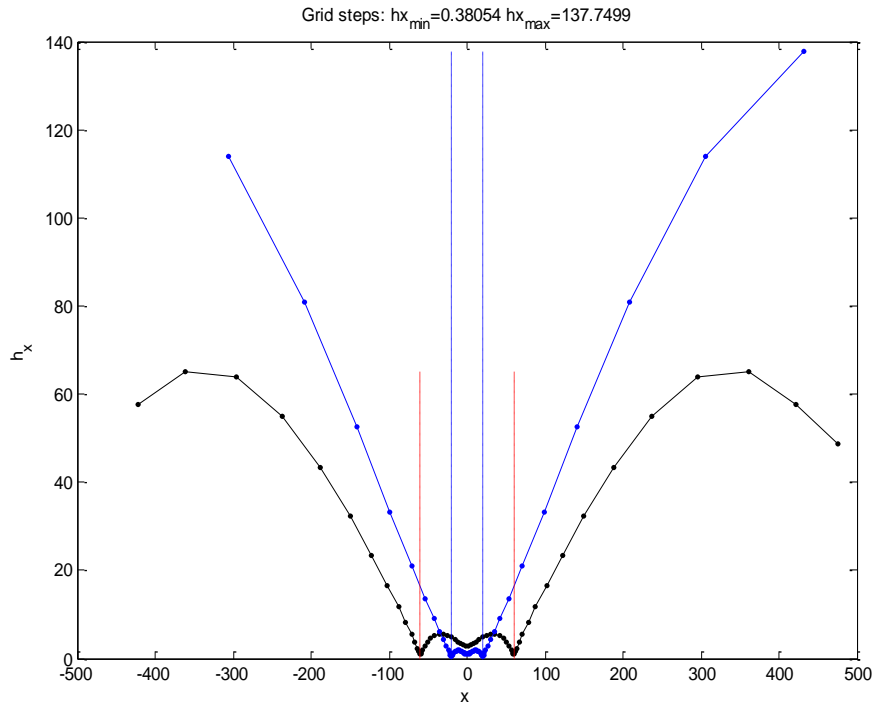


Figure 20. Grid steps $h_x(x)$ when there is no coarsening in x direction, $R_x=1$

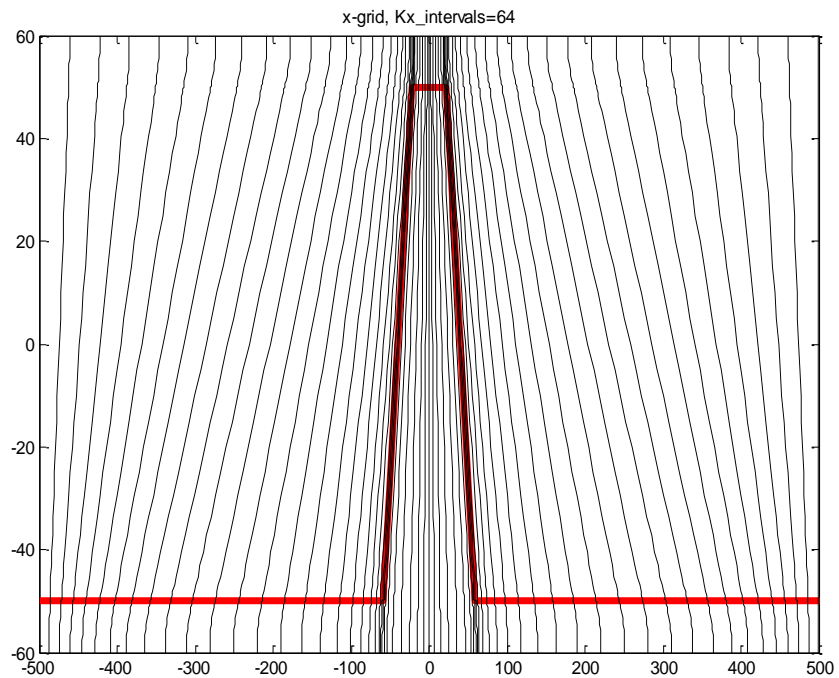


Figure 21. x -grid for coarsening $R_x = 8$

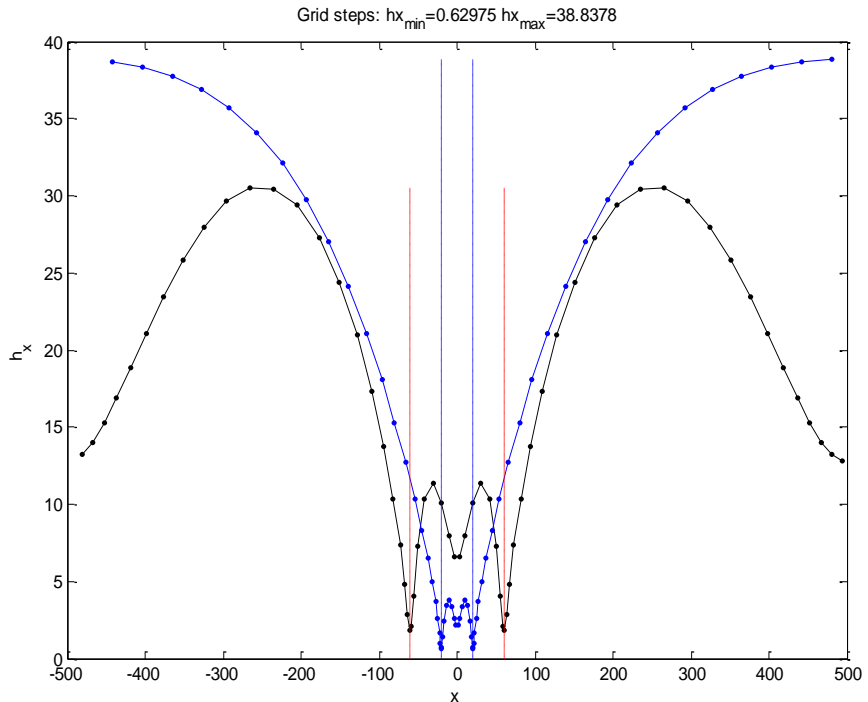


Figure 22. Grid steps $h_x(x)$ for coarsening $R_x = 8$

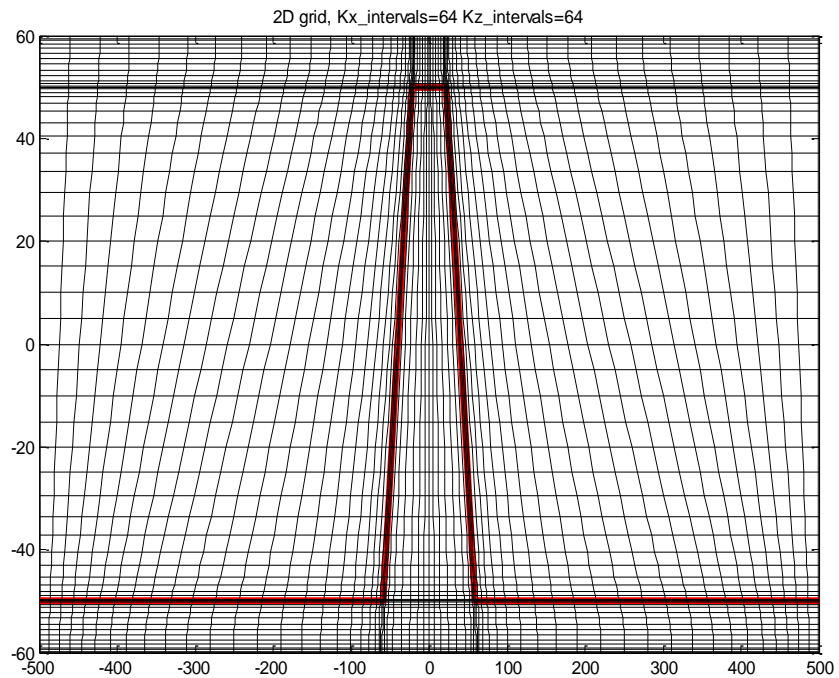


Figure 23. Final grid for $H=120, h_g=100, W=1000,$
 $w_g=80, G_x=0.1, G_z=0.1, R_x=8, R_z=0.125$